Automation of In-Bed Repositioning, Assistance to Sitting, and Transfer for Bedridden Patients via Robot Arms and Strap Interface

by

Kaleb Blake

Submitted to the Department of Mechanical Engineering
in partial fulfillment of the requirements for the degree of

MASTER OF SCIENCE IN MECHANICAL ENGINEERING

at the

MASSACHUSETTS INSTITUTE OF TECHNOLOGY

May 2024

Authored by: Kaleb Blake
Department of Mechanical Engineering
May 20, 2024

Certified by: Harry H. Asada
Professor of Mechanical Engineering, Thesis Supervisor

Accepted by: Nicolas Hadjiconstantinou
Professor of Mechanical Engineering
Graduate Officer, Department of Mechanical Engineering

Automation of In-Bed Repositioning, Assistance to Sitting, and Transfer for Bedridden Patients via Robot Arms and Strap Interface

by

Kaleb Blake

Submitted to the Department of Mechanical Engineering
on May 20, 2024 in partial fulfillment of the requirements for the degree of

MASTER OF SCIENCE IN MECHANICAL ENGINEERING

ABSTRACT

Mobility and immobility as fundamental aspects of a patient's health. There are several factors that contribute to mobility impairments, including various medical conditions and injuries. Prolonged immobility has detrimental effects many of the body's vital organ systems and decreases quality of life in general. Caregivers work to help patient with different levels of mobility perform necessary tasks. Severely immobile or bedridden patients are the most difficult to handle. Caregivers often experience musculoskeletal disorders lifting injuries in their line of work. Assistive devices were made to mitigate this, but their usage in practice is still limited, so caregiver injuries are still prevalent. This thesis presents a new idea that can automate in-bed motion, assistance to seated positions, and transfer for patients with severe immobility. Comfortable straps that wrap around the patient's upper torso and thighs will be held by robot arms. The robot arms will perform movements that can control the torso and thigh angles, hip position in and out of the bed plane, and the normal force the bed provides at the hip. The control techniques described in this paper include closed loop control of a quasi-static formulation of the system and model-reference adaptive trajectory control. The results show there is promise in these methods to automate assistance of bedridden patients.

Thesis supervisor: Harry H. Asada
Title: Professor of Mechanical Engineering

Acknowledgments

I would like to acknowledge my advisor Harry Asada for bringing me into his lab and providing guidance for me in my research.

I would like to acknowledge my family for supporting me throughout my academic journey and showing me the love and care I need.

Contents

List of Figures

Chapter 1

Introduction

1.1 Mobility Overview

Mobility and immobility are fundamental aspects of a patient's health, encompassing the ability to change and control body position. Physical mobility relies on various factors such as muscle strength, skeletal stability, joint function, and neuromuscular coordination. Disruptions to this integrated process can result in impaired mobility or complete immobility. This spectrum ranges from minor limitations, where patients can make significant positional adjustments independently, to severe immobility, where even slight changes require assistance [1]. The concept of being bedridden is a type of severe immobility where the patient has to stay in bed for a long period. It can be described as a terminal state that eventually leads to physical or social death [2].

A prolonged state of immobility can occur due to various reasons, including senility, obesity, accidents, strokes, or spinal injuries [2]. Furthermore, immobility can arise from other diverse physical and psychological factors, including acute and chronic diseases, and chronic pain. In specific, conditions such as osteoarthritis, rheumatoid arthritis, muscular dystrophy, cerebral palsy, multiple sclerosis, and Parkinson's disease can significantly impair mobility. Similarly, traumatic injuries like fractures or head injuries hinder movement. Some chronic diseases that cause fatigue or pain, which diminish a patient's inclination to move, are heart failure, chronic obstructive pulmonary disease, and depression [1].

Prolonged bed rest, whether due to surgery, injury, or illness, contributes to the deterioration of cardiovascular, respiratory, gastrointestinal, and musculoskeletal systems. This can lead to muscle weakness and atrophy, muscle shortening, pressure sores, respiratory issues, circulation problems, and bone demineralization [2]. In fact, muscle loss is estimated at 20% per week of immobility. Not only that but, decreased mobility is a significant risk factor for skin breakdown, as indicated by the Braden Scale [1].

However, promoting mobility can mitigate these complications. There is extensive literature that highlight numerous benefits of mobilization, including reduced delirium, pain, urinary discomfort, urinary tract infections, fatigue, deep vein thrombosis (DVT), and pneumonia. Moreover, mobilization decreases depression, anxiety, and symptom distress while enhancing comfort, satisfaction, quality of life, and independence (Chapter 13 Mobility).

Strategies to enhance patient mobility span two categories: in-bed interventions and out-of-bed interventions. In-bed strategies include repositioning activities, range of motion exercises, and assisting patients to sit on the bed's edge. These are described in more detail in section 1.5. Out-of-bed interventions involve transferring patients from bed to chair and aiding in ambulation, which is the ability to walk [1]. These and other mobility strategies are executed by caregivers [2].

1.2 Caregiver Injury Persistence

Assessing the mobility status and determining the need for assistance are critical components of patient care, particularly in environments where safe patient handling and mobility (SPHM) are paramount. The Banner Mobility Assessment Tool (BMAT) was developed to address this need, serving as a nurse-driven bedside assessment tool. It guides healthcare professionals through a comprehensive four-step functional task list, enabling them to gauge the patient's mobility level accurately. By identifying the patient's capabilities, the BMAT facilitates the selection of appropriate SPHM technology for safe lifting, transferring, and mobilizing the patient.

Safe patient handling is a fundamental aspect of healthcare delivery, especially when assisting individuals with decreased mobility. Over the past decade, there has been a significant emphasis on SPHM in both acute and long-term care settings, resulting in a notable decrease in staff lifting injuries after three decades of steady increase. Despite this progress, nurses continue to experience a higher prevalence of musculoskeletal disorders related to lifting compared to workers in industries like manufacturing and construction.

Traditionally, there was a misconception that lifting injuries could be mitigated through the application of proper body mechanics. However, evidence has challenged this notion. While body mechanics involve the coordinated use of muscles, bones, and the nervous system to maintain balance, posture, and alignment during patient movement, they do not adequately address the complexities of patient lifting scenarios. The National Institute of Occupational Safety and Health (NIOSH) establishes maximum load limits for various lifting activities, taking into account factors such as lifting position, frequency, and duration of exposure.

Patients present unique challenges for lifting due to their irregular shapes, unexpected movements, and potential hindrances like wounds or medical devices. Consequently, the safe lifting load for patients is often less than the maximum recommended load for inanimate objects. Despite efforts to employ proper body mechanics and lifting techniques, lifting injuries persist among nurses, particularly when faced with exertion, awkward postures, prolonged exposure to lifting tasks, and unpredictable patient movements. For instance, tasks that require nurses to maintain awkward positions while exerting force, such as bending over and twisting simultaneously or extended reaching, significantly elevate the risk of injury [1].

1.3 Necessity of Assistive Devices

As mentioned previously, caregiving poses significant physical risks for caregivers, leading to injuries and subsequent absences from work. Assistive technologies play a pivotal role in mitigating these risks and reducing injury rates among caregivers. For instance, the utilization of mechanical lifts, a basic form of assistive technology (more of these are described in section 1.4), has been shown to substantially decrease injury rates and lost workdays among caregivers.

Another significant driver for the adoption of assistive technologies is the financial burden associated with caregiving. In the United States alone, there are an estimated 40 to 50 million people living with disabilities requiring care, as reported by the National Institutes of Health. The cost of caregiving extends beyond the visible expenses incurred in care facilities and hospitals, encompassing hidden costs associated with informal caregiving. As hospitals increasingly resort to outpatient procedures and shorter hospital stays to mitigate rising healthcare expenses, the reliance on family caregivers has surged.

A staggering 61% of caregivers for elderly and disabled family members are employed, highlighting the economic impact of caregiving responsibilities on the workforce. Many caregivers find themselves needing to adjust their work schedules, resulting in wage and income loss, and in some cases, early retirement. This informal caregiving cost is estimated to total at $522 billion a year in the United States. This was measured by estimating income lost during the time that unpaid caregivers spend on eldercare. These financial implications are compounded by the high out-of-pocket healthcare costs associated with caregiving (Review of assistive technologies for bedridden persons).

Not only is it costly, but personal assistance may not directly enhance independence of the patient. On the other hand, technological assistance encompasses the use of specialized equipment that can enable individuals with reduced mobility to carry out activities of daily living (ADLs) with greater autonomy. Research suggests that the implementation of assistive technology for indoor/outdoor mobility, bed transfer, and bathing can result in a 25% reduction in the hours of personal assistance services required. This statistical evidence shows the dual benefits of assistive technology, both in supporting caregivers and enhancing the independence of individuals with disabilities.

In essence, assistive technologies serve as a cost-effective solution to address the multifaceted challenges associated with caregiving. By empowering individuals with disabilities to perform ADLs more independently and alleviating the physical and financial strain on caregivers, these technologies contribute to an improved quality of life for all stakeholders involved [2].

1.4 Basic Assistive Devices

In the realm of safe patient handling and mobility, nurses often utilize various assistive devices tailored to meet individual patient needs. These devices serve to facilitate activities of daily living and enhance patient mobility. Among the arsenal of assistive devices are gait belts, slider boards, sit-to-stand lifts, and mechanical lifts.

Gait belts play a crucial role in ensuring stability during tasks such as standing, ambulation, or transferring from one surface to another. These belts, typically 2 inches wide, are equipped with handles and are secured around the patient's waist with a buckle. It's imperative to apply the gait belt over the patient's clothing or gown to prevent skin abrasions.

Slider boards, also known as transfer boards, serve as aids for moving immobile patients between surfaces while they remain in a supine position. This tool facilitates seamless transfers, such as from a stretcher to a hospital bed. The utilization of slider boards reduces the risk of musculoskeletal strain for both patients and healthcare providers.

Sit-to-stand lifts, alternatively referred to as Sara Lifts, Lift Ups, Stand Assist, or Stand Up Lifts, cater to patients who possess some degree of weight-bearing capacity but lack the strength to transition from sitting to standing independently. These lifts, available in mechanized and non-mechanized variants, provide essential assistance for patients with compromised mobility, enabling them to change positions safely.

Mechanical lifts, characterized by hydraulic mechanisms and slings, are indispensable for patients who are unable to bear weight or assist with movement due to medical conditions or physical limitations. These lifts offer a means of transferring patients with minimal risk of injury to both patients and caregivers. They can be either portable or permanently affixed to the ceiling, offering flexibility and convenience in various healthcare settings.

Each of these assistive devices plays a vital role in promoting patient safety, comfort, and independence during mobility tasks. By incorporating these tools into patient care protocols, nurses can effectively address the diverse mobility needs of individuals under their care, ensuring optimal outcomes and minimizing the risk of adverse events associated with manual handling [1].

1.5 In-Bed Mobility Techniques

1.5.1 In-Bed Repositioning and Moving

Repositioning bedridden patients is a critical aspect of their care, aiming to maintain proper body alignment and prevent complications such as pressure injuries, foot drop, and contractures. This process is particularly essential for patients with decreased mobility due to medical conditions or treatments. Utilizing supportive devices like pillows, rolls, and blankets can enhance comfort and safety during repositioning. Various positions are available based on individual patient factors such as their medical condition, preferences, or treatment needs.

When moving a patient up in bed, it's crucial to assess the level of assistance required for optimal care. Preventing friction and shear during this maneuver is vital to avoid pressure injuries. If the patient cannot assist with repositioning, protocols regarding the use of lifting devices and mechanical lifts should be followed. However, if the patient can contribute to the process, specific guidelines should be adhered to with assistance from another healthcare professional.

Communication with the patient is essential, explaining the process and how they can participate. Proper positioning of the patient in the supine position with appropriate pillow placement helps ensure safety. Utilizing proper body mechanics, such as maintaining a straight back and bending the knees, reduces the risk of back injury for healthcare providers. With coordinated effort and careful movement, the patient is gently slid up the bed, rather than lifted, ensuring smooth transition and minimizing the risk of injury.

Following the repositioning, it's important to readjust the patient for comfort, replace the pillow under their head, and cover them with a sheet or blanket. Lowering the bed, raising side rails as necessary, and ensuring the call light is within reach complete the process. Hand hygiene should be performed to maintain cleanliness and infection control standards, ensuring comprehensive patient care and safety throughout the repositioning procedure [1].

1.5.2 Assisting to a Seated Position

Assisting patients to a seated position is a critical step before ambulation, repositioning, or transferring them between surfaces, such as from a bed to a wheelchair. Moving the patient to the side of the bed prior to these activities helps prevent strain or overreaching by healthcare professionals. Additionally, positioning the patient to the side allows for better proximity to their center of gravity, enhancing balance during handling.

Patients who have been lying in bed for extended periods may experience vertigo or orthostatic hypotension when transitioning to a seated position. Vertigo presents as a sensation of dizziness or spinning, while orthostatic hypotension involves a drop in blood pressure upon sitting or standing, leading to feelings of faintness or lightheadedness. To mitigate these risks, it's advisable to start the transfer or ambulation process by seating the patient on the side of the bed for a few minutes with their legs dangling.

Before assisting the patient, it's essential to communicate with them about the process and ascertain if additional assistance or mechanical lift is required. Ensuring the bed is lowered and locked, the healthcare provider can then proceed with guiding the patient to the seated position on the edge of the bed.

Positioned facing the head of the bed at a 45-degree angle with feet apart, one foot forward, the healthcare provider assists the patient to turn onto their side, facing them, and move closer to the bed's edge. Supporting the patient's shoulders and neck with one hand, they prompt the patient to use their elbows to push up against the bed while grasping the side rail. As the patient sits, the provider shifts their weight from front to back foot to facilitate the movement, avoiding the patient wrapping their arms around their shoulders, which could cause back injuries.

Simultaneously, the provider gently supports the patient's outer thighs with the other hand, assisting them in sliding their feet off the bed to dangle or touch the floor. Maintaining proper body mechanics, such as bent knees and a straight back, is crucial during this process.

Finally, the patient is assessed for symptoms of orthostatic hypotension or vertigo. If any dizziness is observed, the patient is encouraged to remain seated on the edge of the bed until symptoms resolve before proceeding with further activities like transferring or ambulating. This systematic approach prioritizes patient safety and comfort during the transition to a seated position [1].

1.6 Assistive Technology Usage In Practice

While SPHM programs may prevent work-related injuries and associated measures such as lost work days and medical costs, there is conflicting evidence regarding their effectiveness. Moreover, the effectiveness of these programs may vary over time and by patient acuity level.

Despite the implementation of recommended SPHM programs, barriers exist that can impede the adoption of safe patient handling practices in nursing care. Recent studies have aimed to understand the intermediate outcome of the use or lack of use of patient lift and transfer devices, along with factors influencing such use. These influencing factors encompass a wide range of variables, including worker characteristics and experiences, patient characteristics, perceptions related to lift use, equipment availability and accessibility, competing demands, social support, and safety climate. Recognizing and addressing these barriers is crucial for enhancing the effectiveness of SPHM programs and improving patient and worker safety in healthcare settings [3].

The results of the study from [3] revealed that despite nurses and nurse care assistants being trained in equipment use, only 40 percent of the participants utilized equipment for at least half of lifts and transfers. Various factors were identified to be the cause of this, including the patient's inability to assist with the lift or transfer or the patient being of a size or weight that required additional assistance. Speaking of additional assistance, the availability of others who could aid in manual lifting or use of lift equipment were significant factors as well. Ensuring that equipment functioned properly, having necessary supplies available, and ease of retrieval from storage were also important considerations. The study also noted that physical assistance from patients was quite uncommon.

It's essential to recognize that while lifting devices hold the potential to enhance patient safety, their improper use or malfunction can lead to adverse outcomes, including skin-related issues, falls, serious injuries, and even fatalities. Factors contributing to such negative outcomes may include the use of faulty equipment, employing devices incompatible with the patient's characteristics, or incorrect utilization of the equipment. Addressing these safety concerns necessitates adequate caregiver training in the proper use of lift equipment, encompassing formal training, refresher sessions, and regular hands-on practice. Nonetheless, challenges related to time constraints in accessing training opportunities have been identified, indicating a potential barrier to ensuring comprehensive caregiver education in this regard.

Similar behavior is seen in practice for repositioning tasks. Although the adoption of friction-reducing devices or other assistive approaches holds promise in alleviating the physical demands of repositioning tasks, several factors influence healthcare workers' decisions regarding their utilization. These factors include considerations such as time constraints, patient condition, availability and perceived effectiveness of assistive devices, and the number of caregivers required for task completion. Recognizing and addressing these multifaceted influences is crucial for optimizing the effectiveness of repositioning strategies and ensuring the safety and well-being of both patients and healthcare workers [3].

1.7 Advances in Assistive Technology

1.7.1 Commercial Hospital Beds

Hospital beds play an increasingly vital role in enhancing patient comfort, mitigating the adverse effects of prolonged bed rest, and alleviating the burdensome tasks of caregivers. With a broad spectrum of options available on the market, ranging from manual to fully automated high-tech beds, patients and healthcare facilities have ample choices to cater to varying needs. Key global manufacturers such as Linet, Hill-Rom, and Stryker offer diverse solutions in this regard.

The Linet Multicare Bed system boasts a mechanism with six degrees of freedom (DOF). The bed's height can be adjusted, it can tilt to achieve head-up or foot-up positions, and it can rotate the patient as a whole in the transverse plane, facilitating tasks like changing diapers and bed linen. It can also rotate the waist, hip, and knee joints in the sagittal plane.

Each Linet Multicare Bed offers a range of additional features, including an embedded X-ray cassette tray, multiple control panels for both caregiver and patient, bed exit alarms, security fences to prevent falls, built-in weighing functions, and communication devices.

The Hill-Rom TotalCare Connect Bed, Stryker Intouch Bed, and Stiegelmeyer – Vertica Bed provide a similar set of functionalities compared to the Linet Multicare Bed, except they can't rotate the patient in the transverse plane. A unique feature of the TotalCare Connect Bed is its automatic seat deflation, which enables the bed to transition into a chair egress position, ensuring that the patient remains close to the ground for added safety and convenience [2].

1.7.2 Solutions for Moving Patients In and Out of Bed

The AgileLife Patient Transfer System is a commercially available hospital bed that can rotate the patient's lower legs (at the lower end of the bed) in the sagittal plane and move the patient along the length of the bed into a wheelchair via continuous rotation of the belt-like system [2].

The Careful Patient Mover (C-Pam) is a device developed by DAIHEN Corporation that can transfer a patient from a bed to a stretcher or vice verse with no effort from the patient and minimized effort from the nursing staff. When transferring a patient from bed to stretcher, the apparatus navigates from the stretcher across the bed, gently maneuvering underneath the patient lying on the bed. It then elevates the patient slightly and guides them back onto the stretcher. Conversely, when transferring a patient from stretcher to bed, the apparatus moves to the bed and gently lowers the patient onto it [4].

Finger and Asada, developed a novel system that utilizes a wave-like periodic motion generated on the surface of the mattress by activating individual coil springs embedded within. This movement of the mattress surface facilitates the movement of the bedridden patient's body, allowing for translation and rotation within the mattress plane [5].

Another mechanism has been developed for rolling and repositioning bedridden patients by employing a pair of actuated rollers attached to both sides of the bedsheet. This mechanism effectively lifts and manipulates the patient's body, helping to prevent the development of painful bedsores and pneumonia [6].

A different design is that consisting of two beds implemented to facilitate posture adjustment and transferring for bedridden individuals. For posture adjustment, a main bed is designed with four bedplates, which enables the bed to accommodate sitting and leg-lifting motions, facilitating movement of the knees, hips, and waist. For transferring tasks, a nursing bed can transform from being flat to a wheelchair for transportation. Both beds have moving belts, so the bedridden patient can be seamlessly transferred from the main bed to the nursing bed [7].

1.7.3 Lifting Transfer Devices

Toshiyuki Kita developed the Robohelper Sasuke to facilitate the transition of patients from a prone to a sitting position. Sasuke consists of two rods connected by a sling. It can raise the sling and rods in the vertical direction, move the rods towards or away from each other to adjust sling stiffness, and it can rotate the sling to transition the patient to a sitting position, once the patient is lifted and moved away from the bed [2].

The Toyota patient transfer assist robot can transport patients from their bed to different areas like the bathroom or outdoors. The robot features weight-supporting arms along with a wheeled platform. The arms extend out towards the patient and once the patient is secured on the robot, the robot arms can rotate and lift the patient and transport them as needed [2].

1.7.4 Other Devices

The intelligent bed robot system (IBRS) features a specialized bed equipped with two robotic arms and an array of pressure sensors embedded in the mattress. By analyzing the pressure distribution on the mattress, the system estimates the patient's posture and provides appropriate assistance through the robot arms. The bar-type robotic arm can provide gentle, active support to the user when they try to change their body posture. The robotic arm also has a tray mounted on it, which is used to deliver objects to the patient [8].

A novel prototype robot named RIBA has been developed, which feature human-like arms tailored for transferring individuals from a bed to a wheelchair and vice versa. While caregivers oversee environmental monitoring and decision-making, the robot assumes responsibility for executing demanding physical maneuvers. Caregivers convey instructions to the robot through tactile sensors [9].

1.8 Proposed Solution

This thesis proposes a new solution to tackle the need to automate in-bed repositioning tasks as well as assistance to a seated position. Two straps, with similar comfort levels to gait belts, will be wrapped around the patient's upper torso and lower thighs. The position of the free ends of the straps will be controlled to manipulate the patient's body to perform the desired movements. The patient positions that can be controlled include the torso and thigh joint angles in the sagittal plane, the hip location within and outside the plane of the mattress, and the coronal rotation of the whole body. The contact force between the base of the hip and the bed can be controlled as well. In this thesis, said control will be performed by commercial robot arms, however, a different mechanism can be made in the future to control the free ends of the straps. In addition, this thesis assumed that the free ends of each strap are connected to each other respectively, forming two separate closed loops. In the future, this can be changed, though, such that the straps don't form a closed loop and each end of each strap is controlled independently. This would add the possibility of controlling transverse rotation of the patient as in [6] where a bed sheet is used to rotate the patient in the transverse plane. The straps can be thought of as starting on the bed, already underneath the patient, rather than having a caregiver slide them underneath a patient already lying down. In the future, though, this thesis work will be combined with another research project in the same lab, which is focused on creating a strap that can maneuver underneath a patient without the help of a caregiver.

This solution differs from other solutions presented because it has the ability to do both in-bed repositioning and assistance to a seated position all in one. In addition, the solution can be used to transfer a bedridden patient into a wheelchair that is positioned close to the bed. All the other solutions presented can only perform only one or two of these abilities. Not only that, but our solution is fully automated, so the caregiver doesn't have to monitor or help the patient with the movement, aside from attaching the free ends of the straps to the robot arms (or a different mechanism for controlling the straps' free end positions).

In this thesis, the movement of the patient that is focused on is the assistance to a seated position. The desired patient motion for this movement is similar to that described in section 1.5.2. Based on the movement from that section, functional requirements can be specified:

- The bed exerts normal force on the human's hip at all times
- During translation or rotation of the human, it's head, knee, and foot are not in contact with the bed to prevent snagging and excessive resistance
- Minimize hip translation because sliding on your hip is uncomfortable if you have sensitive skin or sores. It also adds excessive resistance
- Rotate the human about the hip to ensure legs are comfortably off the side of the bed or safely on the floor
- Slow, controlled movement of the human to keep the human calm and feel safe

The following figure shows robot arms executing the patient's desired movement on a mannequin.

The following sections will describe the control theory on how to achieve the proposed solution.

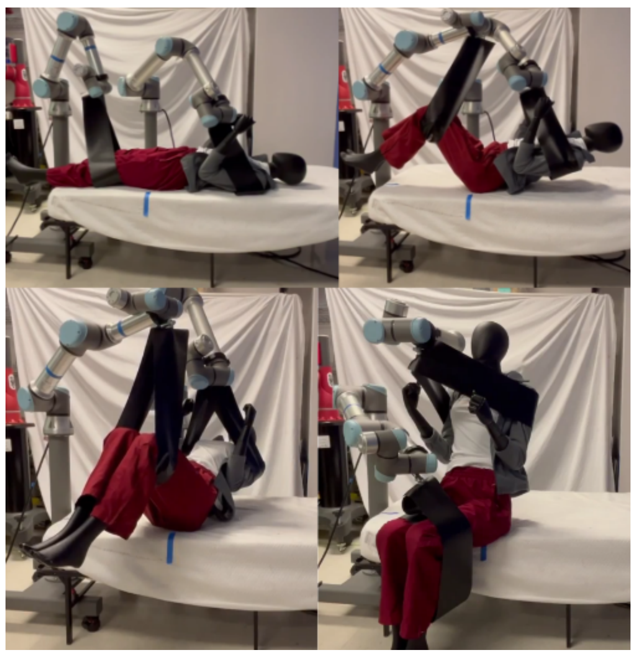

Figure 1.1: Two universal robot arms assisting a mannequin to seated position. The order of the images is from left to right and top to bottom.

Chapter 2

Quasi-Static Control

2.1 Quasi-Static Model Setup

The human is modeled as a simple 3-link structure where rotation is allowed between links, similar to a triple pendulum. Humans have many degrees of freedom and it would be impossible to control all of them with the proposed solution setup. Therefore, this simplified human model with reduced degrees of freedom is used.

There are several assumptions in this system model. The bed is assumed to have the ability to provide a normal force at the hip, while it is assumed that the knee, head, and foot are not in contact with the bed, so the bed is not able to provide normal force at those points. The bed is assumed have linear compliance and damping coefficients and a simple linear compliance equation. The bed is assumed to have a linear static coefficient of friction with the standard static friction equation that depends on normal force applied. The 3-link human is assumed to have linear stiffness and damping between its joints. The straps are assumed to always be in tension, therefore they are modeled as rigid links with constant lengths and relatively small masses compared to the human links. The straps are assumed to be rigidly attached to the 3-link human as well. The straps' respective applied forces to the human torso and thigh links are assumed to be in the same direction as the straps' respective orientations. The robot arms that control the free ends of the straps are assumed to perform high fidelity position control, regardless of the load acting on the robot. This means that the robot end effector can be treated as an ideal source. As such, the robot end effector position qualifies as an input to the system. Since, each robot end effector is coincident with the free end of their respective strap (the end of the strap not in contact with the human), the free ends of the straps also qualify as inputs to the system. Though this is true, the positions of the free ends of the straps are not used as inputs in this model because the straps are assumed to be rigid. Rather, in chapter 3 the free ends of the straps are used as inputs. For this model, the robot arms' applied force are the inputs to the system. The system motion is assumed to be quasi-static at all times, meaning the system is always approximately at equilibrium. The reasoning for this assumption will be revealed in section 2.2.

Though the robot arms are mentioned in the assumptions, the robot arms are not included in the model. This eliminates the closed loop kinematic chain(s) formed by the robot arms, straps, and 3-link human. Avoiding the closed loop kinematic chains in the model removes possibilities of algebraic differential equations in the dynamics, which are difficult to solve. Figure 2.1 the possible closed loop kinematic chains if the robot arms were included in the model.

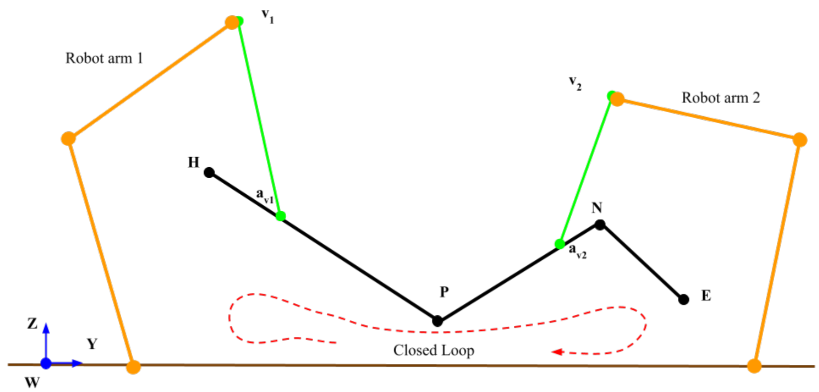

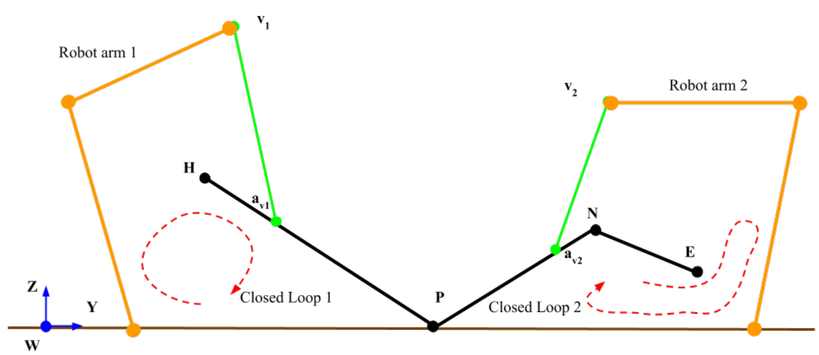

Figure 2.1: Closed loop kinematic chains in the system if the robot arms are included in the model.

The model and control are evaluated in the 2D YZ-plane, rather than the 3D XYZ-plane. This simplification is appropriate since the trajectory to achieve assisting a patient to a seated position can be broken into three 2D trajectories chained together i.e a YZ-plane trajectory is executed first, then a XY-plane trajectory, and lastly a XZ-plane trajectory. The same control strategy can be applied to each plane independently. The 2D system has 7 degrees of freedom (DOF). This comes from 5 links (torso, thigh, and shank links and the two strap links) that have 3 DOF each and 4 revolute joints (at the connections between any two links) which remove 2 DOF each. This leaves 7 DOF. The generalized coordinates of the system can then be specified as $q = [\theta_1, \theta_2, \theta_3, \theta_{v1}, \theta_{v2}, y_P, z_P]^T$. Figure 2.2 shows the kinematics model and figure 2.3 shows the inertial model.

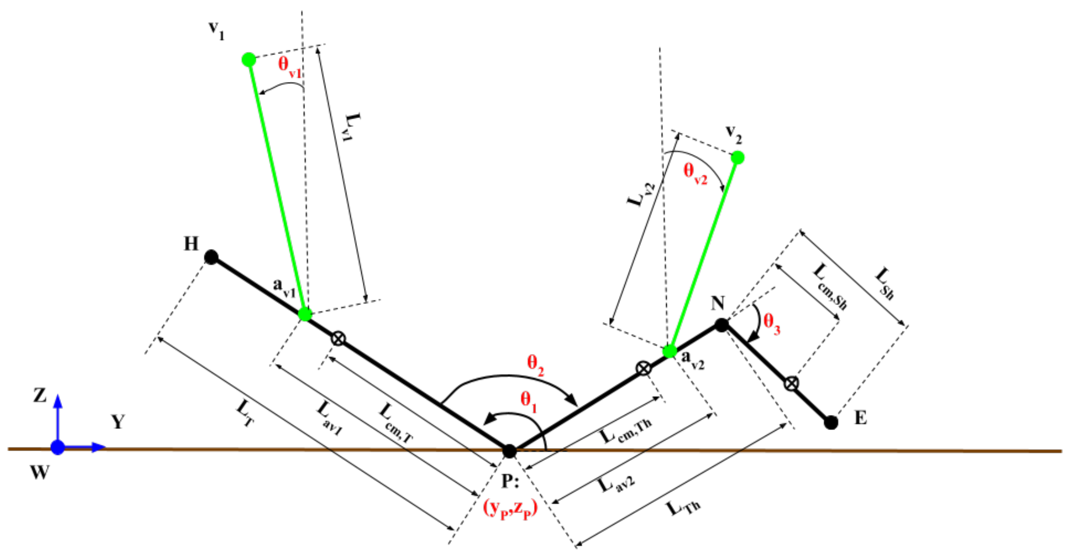

Figure 2.2: 2D kinematic model for quasi-static control. The generalized coordinates have red font.

The world coordinate frame is at W. The black links represent the 3-link human. Link HP is the torso, link PN is the thigh, and link NE is the shank. The green links represent the straps. $\mathbf{F}_{v1}$ and $\mathbf{F}_{v2}$ are the force vectors applied by the robot arms at the free ends of the straps. k_1 and b_1, k_2 and b_2, and k_3 and b_3 are the stiffness and damping coefficients for θ_1, θ_2, and θ_3 respectively. θ_{10}, θ_{20}, and θ_{30} are the neutral locations for the stiffness of θ_1, θ_2, and θ_3 respectively. $F_{bed,z}$ and $F_{fric,y}$ are the normal force and static friction force applied by the bed on the hip of the 3-link human (point P).

From these kinematic and inertial models, the system dynamics can be achieved in the form of $H(\mathbf{q})\ddot{\mathbf{q}} + C(\mathbf{q}, \dot{\mathbf{q}})\dot{\mathbf{q}} + B\dot{\mathbf{q}} + \mathbf{V}_{gk}(\mathbf{q}) = \mathbf{Q}_{nb}(\mathbf{F}_{v1}, \mathbf{F}_{v2})$. $H(\mathbf{q})$ is the inertial terms matrix, $C(\mathbf{q}, \dot{\mathbf{q}})$ is the coriolis/centripetal matrix, B is the damping and friction terms matrix, $\mathbf{V}_{gk}(\mathbf{q})$ is the potential energy vector, and $\mathbf{Q}_{nb}$ is the generalized force vector with no damping or

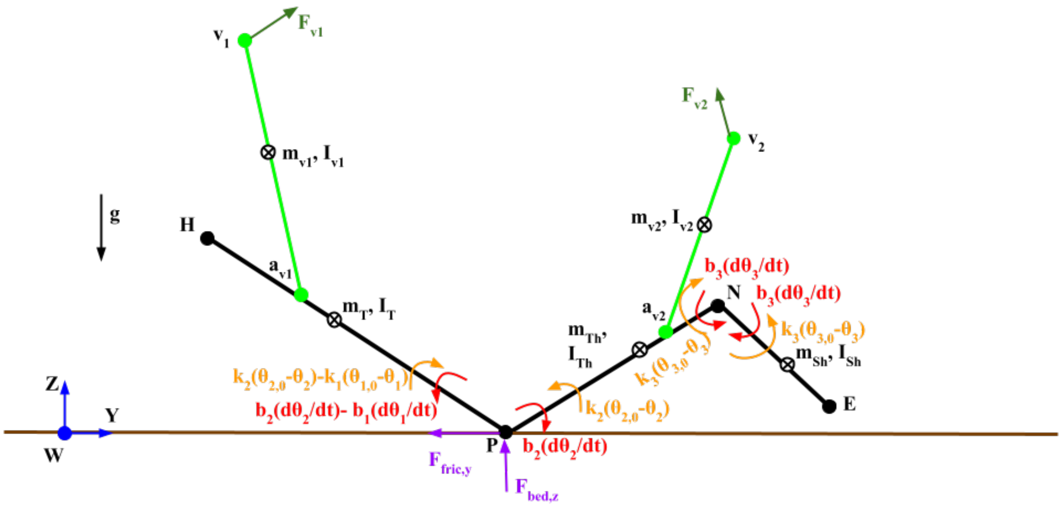

Figure 2.3: 2D inertial model for quasi-static control.

friction terms (since they are included in B). $\mathbf{Q}_{nb}$ is dependent on $\mathbf{F}_{v1}$ and $\mathbf{F}_{v2}$.

2.2 Open Loop Control

If the robot arms are locked in some position, meaning point v_1 and point v_2 (free ends of the straps) from the model are locked in position, the 3-link human will assume some equilibrium position after some period of time. This idea is used to control the generalized coordinates of the system model. It was mentioned in section 2.1 that the system motion is assumed to be quasi-static at all times. Using this assumption, it is possible to know the values of the generalize coordinates of the system given the position of points v_1 and v_2. The reverse is also true. It is possible to know the positions of points v_1 and v_2, if the desired values of the generalized coordinates are given. This statement can be even stronger, though, since not all the generalized coordinates are needed for the previous statement to be true. In fact, given $\theta_1, \theta_2, y_p, z_p$ and $F_{bed,z}$ it is possible to find θ_{v1}, θ_{v2}. θ_{v1}, θ_{v2} can then be used to find $y_{v1}, z_{v1}, y_{v2}, z_{v2}$, which characterize the positions of points v_1 and v_2. $F_{bed,z}$ is included because that is one of the values to control as stated in 1.8. $\theta_1, \theta_2, y_p, z_p$ and $F_{bed,z}$ will be called the decision variables.

The first step to show this is true is to perform free body diagram (FBD) analysis of each link. This is essential in determining the position of the system in equilibrium. The quasi-static assumption allows the sum of forces or moments for every free body diagram to be zero. The free body diagrams for each component of the system can be seen in Figures 2.4, 2.5, 2.6, 2.7, and 2.8 below.

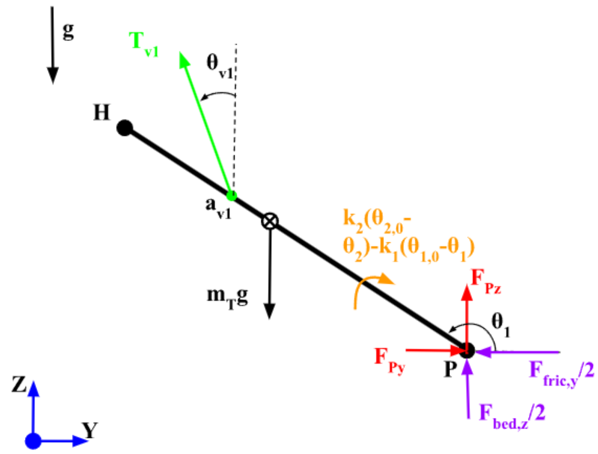

Figure 2.4: Torso FBD

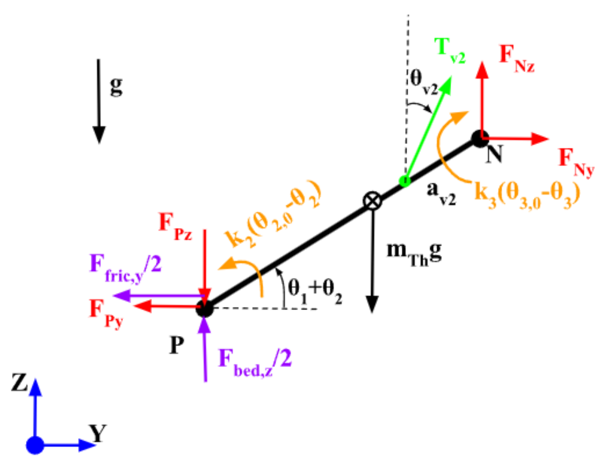

Figure 2.5: Thigh FBD

Using these FBDs, the following system of equations can be formed

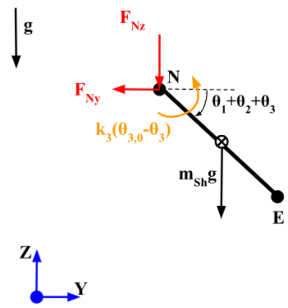

Figure 2.6: Shank FBD

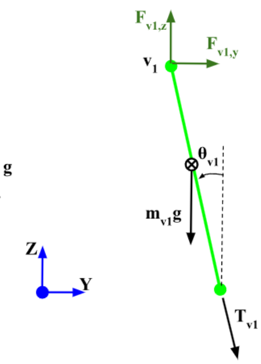

Figure 2.7: Strap 1 FBD

from torso FBDs:

$$\sum F_z : F_{pz} - m_T g + F_{bed,z}/2 + T_{v1} cos(\theta_{v1}) = 0 \quad (1)$$

$$\sum F_y : F_{py} - T_{v1} sin(\theta_{v1}) - F_{fric,y}/2 = 0 \quad (2)$$

$$\sum M_x(a_{v1}) : cos(\theta_1)[m_T g(L_{av1} - L_{cm,T}) - L_{av1}(F_{pz} + F_{bed,z}/2)] + (F_{py} - F_{fric,y}/2)L_{av1} sin(\theta_1) - k_2(\theta_{20} - \theta_2) + k_1(\theta_{10} - \theta_1) = 0 \quad (3)$$

from thigh FBDs:

$$\sum F_z : -F_{pz} + F_{bed,z}/2 - m_{Th} g + T_{v2} cos(\theta_{v2}) + F_{Nz} = 0 \quad (4)$$

$$\sum F_y : -F_{py} - F_{fric,y}/2 - T_{v2} sin(\theta_{v2}) + F_{Ny} = 0 \quad (5)$$

$$\sum M_x(a_{v2}) : cos(\theta_{12})[m_{Th} g(L_{av2} - L_{cm,Th}) + L_{av2}(F_{pz} - F_{bed,z}/2) + F_{Nz}(L_{Th} - L_{av2})] - sin(\theta_{12})[(F_{py} + F_{fric,y}/2)L_{av2} + F_{Ny}(L_{Th} - L_{av2})] + k_2(\theta_{20} - \theta_2) - k_3(\theta_{30} - \theta_3) = 0 \quad (6)$$

where $\theta_{12} = \theta_1 + \theta_2$

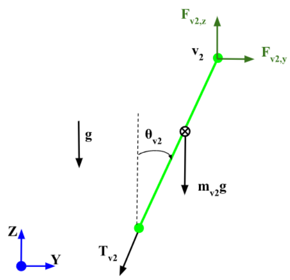

Figure 2.8: Strap 2 FBD

from shank FBDs:

$$\sum F_z : F_{Ny} = 0 \tag{7}$$

$$\sum F_y : -F_{Nz} - m_{Sh}g = 0 \tag{8}$$

There are 8 equations and 8 unknowns $(\theta_{v1}, \theta_{v2}, T_{v1}, T_{v2}, F_{py}, F_{pz}, F_{Ny}, F_{Nz})$, so we can solve for θ_{v1} and θ_{v2}. The formulation below shows how to calculate θ_{v1} and θ_{v2}

$$\begin{aligned}\begin{bmatrix} F_{py} \\ F_{pz} \end{bmatrix} &= A(\theta_1, \theta_2)^{-1}\mathbf{b}(\theta_1, \theta_2, F_{bed,z}) \\ \theta_{v1} &= tan^{-1}(\frac{F_{py}}{m_T g - F_{pz} - F_{bed,z}/2}) \\ \theta_{v2} &= tan^{-1}(\frac{F_{py}}{m_{Th} g + F_{pz} - F_{bed,z}/2 + m_{Sh} g})\end{aligned}$$

The contents of A and b are as follows:

$$A = \begin{bmatrix} L_{av1} sin(\theta_1) & -L_{av1} cos(\theta_1) \\ -L_{av2} sin(\theta_1 + \theta_2) & L_{av2} cos(\theta_1 + \theta_2) \end{bmatrix}$$

$$b = \begin{bmatrix} -m_T g(L_{av1} - L_{cm,T})c_1 + 0.5F_{bed,z} L_{av1} c_1 + 0.5F_{fric,y} L_{av1} s_1 + k_2(\theta_{20} - \theta_2) - k_1(\theta_{10} - \theta_1) \\ 0.5F_{fric,y} L_{av2} s_{12} + 0.5F_{bed,z} L_{av2} c_{12} - m_{Th} g(L_{av2} - L_{cm,Th})c_{12} - k_2(\theta_{20} - \theta_2) + k_3(\theta_{30} - \theta_3) \end{bmatrix}$$

A is invertible if $\theta_2 \neq 0$. This occurs if the torso is folded over the thigh or vice verse.

The next step is to use the kinematics of the system to find the locations of the free ends of the vines y_{v1}, z_{v1}, y_{v2}, and z_{v2} given the desired decision variables and θ_{v1} and θ_{v2}, which were solved for using the desired decision variables. Looking at Figure 2.2, it can be seen that finding y_{v1}, z_{v1}, y_{v2}, and z_{v2} is straightforward and given by the following equations:

$$
\begin{aligned}
y_{v1} &= y_p + L_{av1}cos(\theta_1) + L_{v1}sin(\theta_{v1}) \\
z_{v1} &= z_p + L_{av1}sin(\theta_1) + L_{v1}cos(\theta_{v1}) \\
y_{v2} &= y_p + L_{av2}cos(\theta_1 + \theta_2) - L_{v2}sin(\theta_{v2}) \\
z_{v2} &= z_p + L_{av2}sin(\theta_1 + \theta_2) + L_{v2}cos(\theta_{v2})
\end{aligned}
$$

The choice generalized coordinates that can uniquely define the system is the key to finding these simple kinematic definitions of the free ends of the vine given the other generalized coordinates. For instance, if $\theta_{v1}, \theta_{v2}, y_P$, and z_P were not included in the generalized coordinates and instead y_{v1}, z_{v1}, y_{v2}, and z_{v2} were included, the generalized coordinates would no longer be able to uniquely define the system. In this case, θ_{v1} and θ_{v2} or y_P and z_P would be able to have any value even if $\theta_1, \theta_2, \theta_3, y_{v1}, z_{v1}, y_{v2}$, and z_{v2} were given.

Since, θ_3 is not included in the decision variables and it is not solved for in the above formulation, how is it controlled? θ_3 is actually not directly controlled because there is no generalized force component that has an impact on θ_3. Controlling the angle of the shank is not important for repositioning, assisting to seated positions, or transfer because if the torso and thigh positions are controlled to be at appropriate positions the shank will inherently be in an appropriate position. In fact, the shank moment about point N can be used to solve for θ_3 given θ_1 and θ_2, which are part of the decision variables. Therefore, θ_3 can be checked to make sure it is at appropriate values for every desired θ_1 and θ_2 value, if necessary.

$$-m_{Sh} g L_{cm,Sh} cos_{123} + k_3(\theta_{30} - \theta_3) = 0$$

This concludes the open loop formulation for the quasi-static system. If desired decision variables $(\theta_1, \theta_2, y_p, z_p, F_{bed,z})$ are given, positions of point v_1 and v_2 can be found that will cause the system to achieve the specified decision variables in steady-state (equilibrium).

2.3 Closed Loop Control

The control can be improved by closing the loop. The idea is to modify the desired values for y_{v1}, z_{v1}, y_{v2}, and z_{v2} based on the discrepancy between the measured decision variables and the desired decision variables (decision variable error). The decision variable error, the derivative of the decision variable error, and the integral of the decision variable error over time can be scaled by constants. These constants can be viewed as PID constants. After scaling the various errors by PID constants, the errors in decision variables can then be transformed by the Jacobian of the strap free end with respect to the decision variables: J_{rv1} and J_{rv2}. This creates values that are appropriate to use for changing the desired values of the free ends of the straps. The mathematical definition of the Jacobians can be seen in the equations below.

$$\mathbf{d}_{vars} = [\theta_1, \theta_2, y_p, z_p, F_{bed,z}]^T$$
$$\mathbf{r}_{v1} = [0, y_{v1}, z_{v1}]^T$$
$$\mathbf{r}_{v2} = [0, y_{v2}, z_{v2}]^T$$
$$J_{rv1} = \frac{d\mathbf{r}_{v1}}{d\mathbf{d}_{vars}}$$
$$J_{rv2} = \frac{d\mathbf{r}_{v2}}{d\mathbf{d}_{vars}}$$

A block diagram that illustrates the closed loop is shown in Figure 2.9.

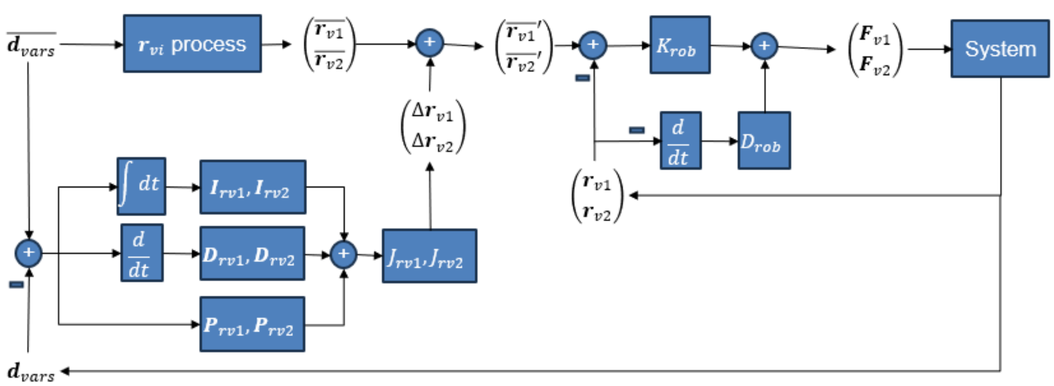

Figure 2.9: Block diagram of quasi-static closed loop control.

$\mathbf{r}_{vi}$ process is the open loop control from section 2.2. $\mathbf{d}_{vars}$ are the measured decision variables and $\overline{\mathbf{d}_{vars}}$ are the desired decision variables. $\mathbf{r}_{vi} = [0, y_{vi}, z_{vi}]^T$ represents the measured value for point v_i. $\overline{\mathbf{r}_{v1}}$ and $\overline{\mathbf{r}_{v2}}$ are the desired values for point v_1 and point v_2 respectively. $\overline{\mathbf{r}_{v1}}'$ and $\overline{\mathbf{r}_{v2}}'$ are the edited desired values for point v_1 and point v_2 respectively. $\mathbf{P}_{rvi}$, $\mathbf{I}_{rvi}$, and $\mathbf{D}_{rvi}$ are constant vectors that have the same length as $\mathbf{d}_{vars}$. Each of those constant vectors are component multiplied with $\mathbf{d}_{vars} - \overline{\mathbf{d}_{vars}}$. J_{rvi} are matrices though, so matrix multiplication is applied at that step. The K_{rob} and D_{rob} section of the block diagram relates to how to robot arm applied force is represented in simulation. This is explain more in depth in section 2.4.

2.4 Simulation Setup

The simulation is performed in MATLAB. The equations of motion are symbolically determined and implemented as a function. Other useful function like the Jacobians of certain position or velocity vectors with respect to the decision variables or generalized coordinates are also computed symbolically.

The dynamic equations of the system include the force applied by the robot arms as the input to the system. In the MATLAB simulation, that force must be provided as an input to the equations of motion in order to propagate the simulation accurately. The simulation uses a virtual constraint force approach. The force applied to the free ends of the vines is that of a virtual spring and damper being attached to the vine free end's current position and the desired position of the vine free end. The virtual spring is setup such that the vines free end is being pulled toward its desired position. The K_{rob} and D_{rob} section of the block diagram represents the virtual spring damper constraint and how the input force is generated for the system. K_{rob} and D_{rob} are the spring and damper constants of the virtual spring constraint. The diagram of the virtual spring and damper can be seen below (Figure 2.10).

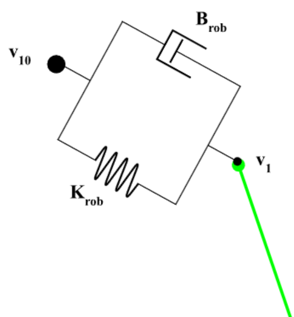

Figure 2.10: Diagram of virtual spring and damper, which generates the input force for the quasi-static system. v_{10} is the desired location of v_1

The dynamics in the simulation are propagated in the following way:

$$\dot{q}_{i+1} = \dot{q}_i + \ddot{q}_i \Delta t$$
$$q_{i+1} = q_i + \dot{q}_{i+1} \Delta t = \dot{q}_i \Delta t + \ddot{q}_i \Delta t^2$$

This ensures that the position propagation correctly includes the acceleration and velocity from the current time step. An image showing a snapshot of the animation for the simulation can be seen in Figure 2.11.

2.5 Results

The test that was conducted was the first step in an automated assistance to seated position motion, which is raising the torso and thigh off the bed from being flat on the bed while keeping y_P and z_P constant and maintaining $F_{bed,z}$ at a constant positive value. Desired θ_1

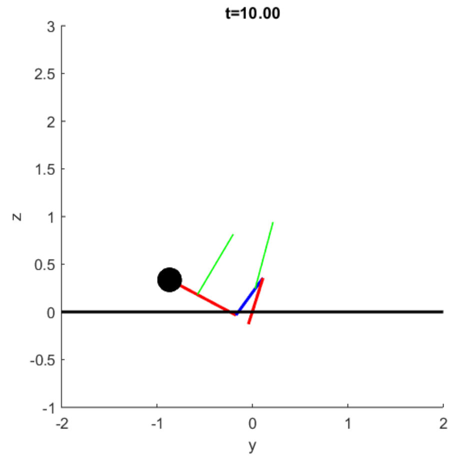

Figure 2.11: Quasi-Static Simulation Animation

goes from 180 degrees to 150 degrees in nine seconds at a constant speed and stays at 150 degrees for 1 second. Desired θ_2 goes from -160 degrees to -90 degrees in nine seconds at a constant speed and stays at -90 degrees for one second. Desired y_P is zero for all time. Desired $F_{bed,z}$ is 10N for all time and desired z_P is desired $F_{bed,z}/K_{bed}$. Initial conditions matched desired values of decision variables at time 0. The figures below show the results of this procedure for the open loop and closed loop cases.

As seen in Figures 2.12 and 2.13 the closed loop control does better than the open loop control because the mean squared error for all decision variables in closed loop control is less than that of open loop control. Mean squared error for $F_{bed,z}$ in both control schemes is much higher than that of other decision variables, which makes sense because force control is much more erratic and difficult to achieve than position control. More research needs to be done to improve the tracking of desired $F_{bed,z}$.

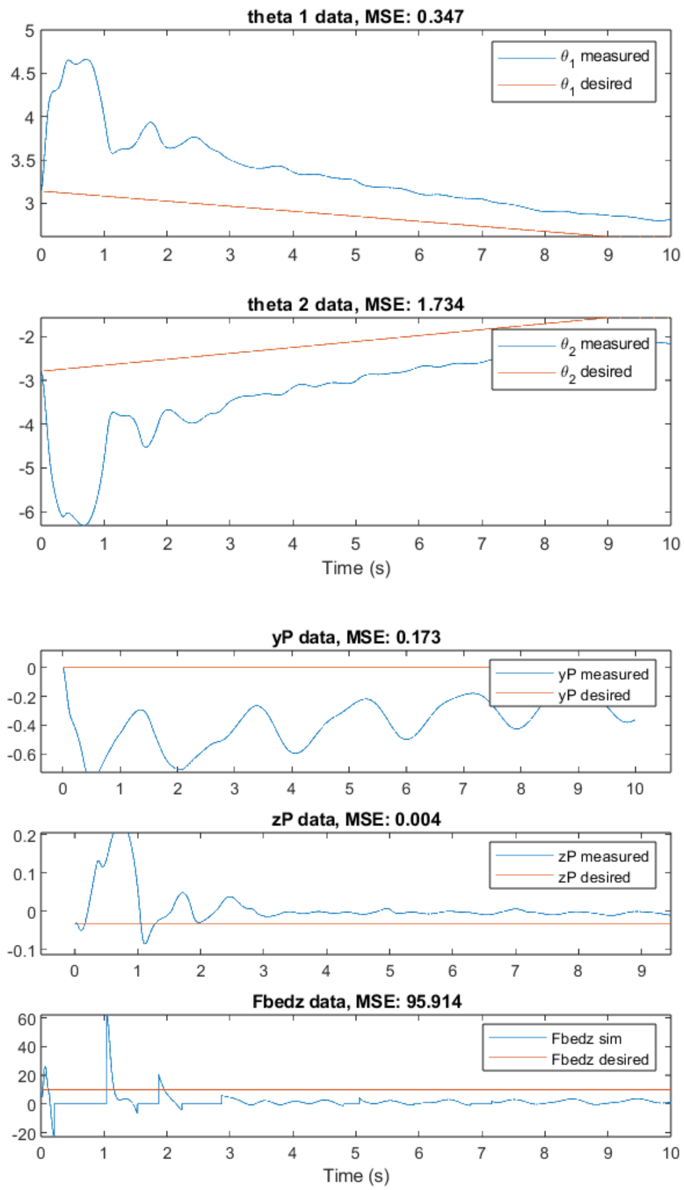

Figure 2.12: Quasi-static open loop results. Mean squared error is shown at the top of each graph.

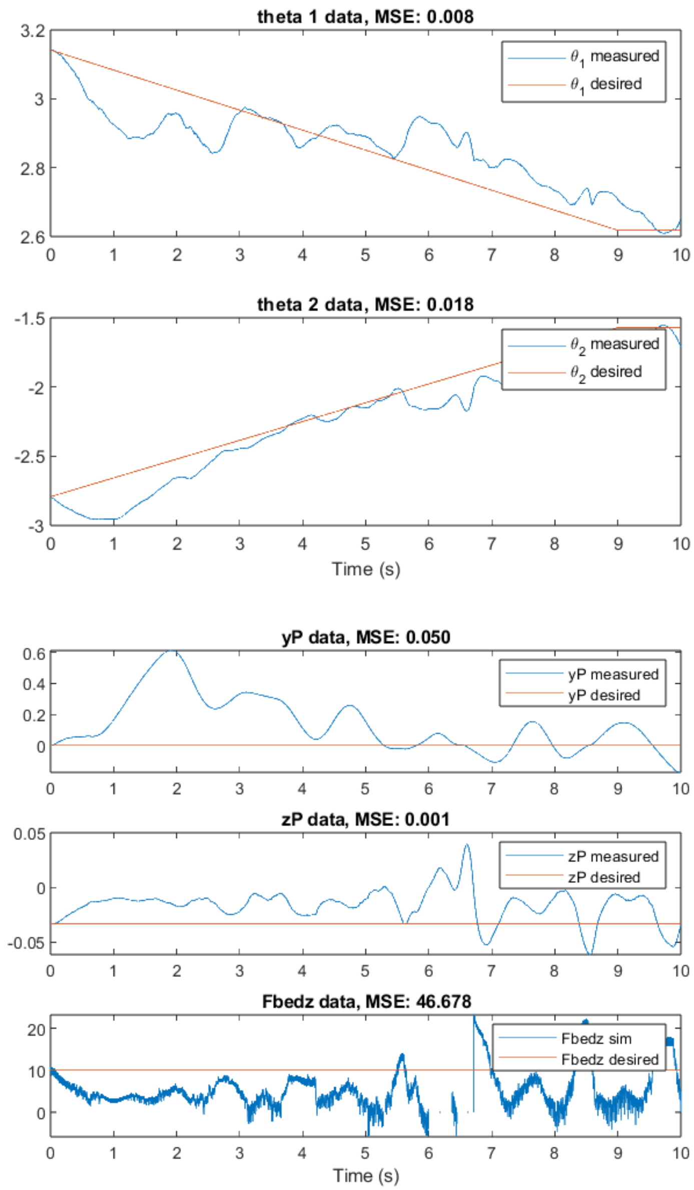

Figure 2.13: Quasi-static closed loop results. Mean squared error is shown at the top of each graph.

Chapter 3

Adaptive Control

3.1 Updated Model

Instead of assuming the straps are rigid, let the model change to assume the straps are elastic with linear compliance equations. In addition, assume the straps have negligible mass compared to the human. As mentioned in section 2.1, the robot arms that control the free ends of the straps are assumed to perform high fidelity position control, regardless of the load acting on the robot. This means that the robot end effector can be treated as an input to the system. In turn, the free ends of the straps also qualify as inputs to the system. With the updated assumption of the strap being elastic, the free ends of the straps can be used as inputs to the system. This is beneficial because position control of the robot arms is more accurate and reliable than force control. Because the straps are elastic, enforcing a position of the free end of the strap will create a force at the interface between the vine and the human that is proportional to the length of the elastic strap (or change in length from the elastic strap's unstretched length). In this way, position of the free ends of the straps corresponds to a input force on the 3-link human. Now the straps can be abstracted away and their effect on the human can be represented with external forces T_{v1} and T_{v2}. The updated inertial model is shown in Figure 3.1. The generalized coordinates of this model are now $\mathbf{q} = [\theta_1, \theta_2, \theta_3, y_p, z_p]^T$.

3.2 Adaptive Control Setup

There are many simplifications made in the model such as reducded human DOFs, linearities in human stiffness and damping, and linear bed friction. There also may be uncertainties in parameters like mass, inertia, center of mass location, and damping coefficients since these are difficult to measure on an actual human. For these reasons, a new approach using adaptive control is explored. Adaptive control can allow the control scheme will work on the real human despite model simplifications and parameter uncertainties. The idea is to use an adaptive control law on the position of the free ends of the straps such that the 3-link human joints' position and velocity are at their desired values.

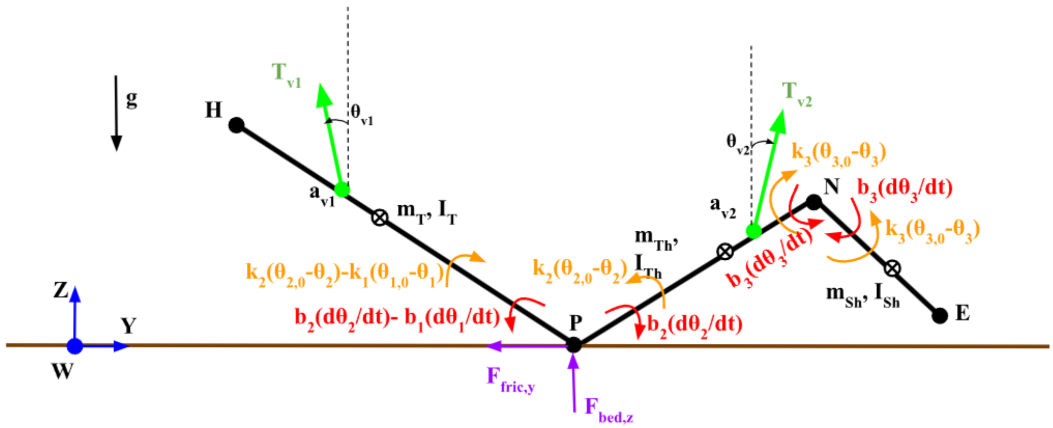

Figure 3.1: New inertial model for the system with the elastic strap assumption

The adaptive control techniques proposed are from the textbook by Slotine and Li [10]. There are two main versions of adaptive control: Model-Reference Adaptive Control and Self-Tuning Control. The control of this system requires Model-Reference Adaptive Trajectory Control because tracking control and on-line parameter estimation are necessary. A block diagram of this type of adaptive control is seen in Figure 3.2.

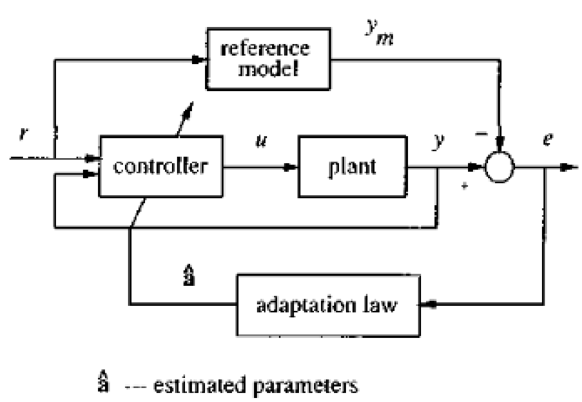

Figure 3.2: Block diagram for basic Model-Reference Adaptive Trajectory Control [10]

For this formulation the nonlinear plant is the 3-link human dynamics based on Figure 3.1. The plant structure is assumed to be known, while the parameters may be unknown. The reference model would be the desired trajectory. Comparing this statement to the block diagram of Figure 3.2 would mean $y_m = r$. The nonlinear plant dynamics are as follows:

$$H(\mathbf{q})\ddot{\mathbf{q}} + C(\mathbf{q},\dot{\mathbf{q}})\dot{\mathbf{q}} + B\dot{\mathbf{q}} + \mathbf{V}_{gk}(\mathbf{q}) = \mathbf{Q}_{nb}(\mathbf{q}, T_{v1}, T_{v2}, \theta_{v1}, \theta_{v2}))$$

where $H(\mathbf{q})$ is the inertial terms matrix, $C(\mathbf{q},\dot{\mathbf{q}})$ is the coriolis/centripetal matrix, B is the damping and friction terms matrix, $\mathbf{V}_{gk}(\mathbf{q})$ is the potential energy vector, and $\mathbf{Q}_{nb}$ is the generalized force vector with no damping or friction terms (since they are included in B). $\mathbf{Q}_{nb}$ is dependent on $\mathbf{q}$, T_{v1}, T_{v2}, θ_{v1}, and θ_{v2}. $T_{v1} = |\mathbf{T}_{v1}|$ and $T_{v2} = |\mathbf{T}_{v2}|$. θ_{v1} and θ_{v2} are the angles of $\mathbf{T}_{v1}$ and $\mathbf{T}_{v2}$, respectively, measured from the z-axis.

The coriolis/centripetal matrix must be formulated carefully in order to preserve conservation of energy of the system:

$$
\begin{aligned}
\frac{d}{dt}(\text{Kinetic Energy}) &= \text{Power into the system (from } \textit{external} \text{ forces)} \\
\frac{1}{2}\frac{d}{dt}(\dot{\mathbf{q}}^T H(\mathbf{q})\dot{\mathbf{q}}) &= \dot{\mathbf{q}}^T(\mathbf{Q}_{nb} - \mathbf{V}_{gk}(\mathbf{q}) - B\dot{\mathbf{q}}) \\
\dot{\mathbf{q}}^T H(\mathbf{q})\ddot{\mathbf{q}} + \frac{1}{2}\dot{\mathbf{q}}^T \dot{H}(\mathbf{q})\dot{\mathbf{q}} &= ... \\
\dot{\mathbf{q}}^T(\mathbf{Q}_{nb} - C(\mathbf{q},\dot{\mathbf{q}})\dot{\mathbf{q}} - B\dot{\mathbf{q}} - \mathbf{V}_{gk}(\mathbf{q})) + \frac{1}{2}\dot{\mathbf{q}}^T \dot{H}(\mathbf{q})\dot{\mathbf{q}} &= ... \\
\forall \mathbf{q},\dot{\mathbf{q}} \quad \dot{\mathbf{q}}^T(\dot{H}(\mathbf{q}) - 2C(\mathbf{q},\dot{\mathbf{q}}))\dot{\mathbf{q}} &= 0
\end{aligned}
$$

This can be understood as $\dot{H} - 2C$ being skew symmetric or $\dot{H} = C + C^T$. The Coriolis matrix is not unique, so to ensure that $\dot{H} - 2C$ is skew symmetric, the following equation was used to find the Coriolis matrix based on the inertial matrix H.

$$c_{ij} = \frac{1}{2}\dot{H}_{ij} + \frac{1}{2}\sum_{k=1}^{n}\left(\frac{\partial H_{ik}}{\partial q_j} - \frac{\partial H_{jk}}{\partial q_i}\right)\dot{q}_k$$

3.3 Model-Reference Adaptive Trajectory Control with a Sliding Variable and Linearly Parameterized Plant Dynamics

In order to execute Model-Reference Adaptive Trajectory Control a sliding variable must be defined, $\mathbf{s}$. This simplifies the problem to a first-order problem instead of a second-order problem. $\mathbf{s} = \dot{\tilde{\mathbf{q}}} + \lambda\tilde{\mathbf{q}}$, where $\tilde{\mathbf{q}} = \mathbf{q} - \mathbf{q}_d$ and $\mathbf{q}_d$ is the desired value of $\mathbf{q}$. Also, $\mathbf{s} = \dot{\mathbf{q}} - \dot{\mathbf{q}}_r$, where $\dot{\mathbf{q}}_r = \dot{\mathbf{q}}_d - \lambda\tilde{\mathbf{q}}$.

Now a Lyapunov function, V, can be constructed:

$$
\begin{aligned}
&V = \frac{1}{2}\mathbf{s}^T H(\mathbf{q})\mathbf{s} + \frac{1}{2}\tilde{\mathbf{a}}^T P^{-1}\tilde{\mathbf{a}} \\
&V > 0 \;\forall\; \mathbf{s},\tilde{\mathbf{a}} \neq 0;\; V = 0 \text{ when } \mathbf{s},\tilde{\mathbf{a}} = \mathbf{0}
\end{aligned}
$$

where $\tilde{\mathbf{a}} = \hat{\mathbf{a}} - \mathbf{a}$, $\mathbf{a}$ is a vector of values determined only by the system parameters and $\hat{\mathbf{a}}$ is an estimate of $\mathbf{a}$. P^{-1} is a constant, symmetric positive definite matrix.

$$
\begin{aligned}
\dot{V} &= \mathbf{s}^T H(\mathbf{q})\dot{\mathbf{s}} + \frac{1}{2}\mathbf{s}^T \dot{H}(\mathbf{q})\mathbf{s} + \dot{\hat{\mathbf{a}}}^T P^{-1}\tilde{\mathbf{a}} \\
&= \mathbf{s}^T H(\mathbf{q})(\ddot{\mathbf{q}} - \ddot{\mathbf{q}}_r) + \frac{1}{2}\mathbf{s}^T \dot{H}(\mathbf{q})\mathbf{s} + \dot{\hat{\mathbf{a}}}^T P^{-1}\tilde{\mathbf{a}} \\
&= \mathbf{s}^T(\mathbf{Q}_{nb}(\mathbf{q}, T_{v1}, T_{v2}, \theta_{v1}, \theta_{v2})) - C(\mathbf{q}, \dot{\mathbf{q}})\dot{\mathbf{q}} - B\dot{\mathbf{q}} - \mathbf{V}_{gk}(\mathbf{q}) - H(\mathbf{q})\ddot{\mathbf{q}}_r) \\
&\qquad + \frac{1}{2}\mathbf{s}^T(2C(\mathbf{q}, \dot{\mathbf{q}}) + \text{skew symmetric})\mathbf{s} + \dot{\hat{\mathbf{a}}}^T P^{-1}\tilde{\mathbf{a}} \\
&= \mathbf{s}^T(\mathbf{Q}_{nb}(\mathbf{q}, T_{v1}, T_{v2}, \theta_{v1}, \theta_{v2})) - H(\mathbf{q})\ddot{\mathbf{q}}_r - C(\mathbf{q}, \dot{\mathbf{q}})\dot{\mathbf{q}}_r - B\dot{\mathbf{q}} - \mathbf{V}_{gk}(\mathbf{q})) + \dot{\hat{\mathbf{a}}}^T P^{-1}\tilde{\mathbf{a}} \\
&= \mathbf{s}^T(\mathbf{Q}_{nb} - Y(\ddot{\mathbf{q}}_r, \dot{\mathbf{q}}_r, \dot{\mathbf{q}}, \mathbf{q})\mathbf{a}) + \dot{\hat{\mathbf{a}}}^T P^{-1}\tilde{\mathbf{a}}
\end{aligned}
$$

Matrix $Y(\ddot{\mathbf{q}}_r, \dot{\mathbf{q}}_r, \dot{\mathbf{q}}, \mathbf{q})$ and vector $\mathbf{a}$ are constructed such that $Y\mathbf{a} = H(\mathbf{q})\ddot{\mathbf{q}}_r + C(\mathbf{q}, \dot{\mathbf{q}})\dot{\mathbf{q}}_r + B\dot{\mathbf{q}} + \mathbf{V}_{gk}(\mathbf{q})$. It turns out that the parameters are linearly involved in the plant dynamics. $\mathbf{a}$ is found to be:

$$
\mathbf{a} = \begin{bmatrix}
m_T L_{cm,T}^2 + I_T \\
m_{Th} L_{cm,Th}^2 + I_{Th} + m_{Sh} L_{Th}^2 \\
m_{Sh} L_{cm,Sh}^2 + I_{Sh} \\
m_{Sh} L_{Th} L_{cm,Sh} \\
m_T L_{cm,T} \\
m_{Th} L_{cm,Th} + m_{Sh} L_{Th} \\
m_{Sh} L_{cm,Sh} \\
m_T + m_{Th} + m_{Sh} \\
b_1 \\
b_2 \\
b_3 \\
\mu_{k,bed} \\
k_1 \\
k_2 \\
k_3
\end{bmatrix}
$$

and the Y matrix is as follows:

$$
Y = \begin{bmatrix}
\mathbf{Y}_1 \\
\mathbf{Y}_2 \\
\mathbf{Y}_3 \\
\mathbf{Y}_4 \\
\mathbf{Y}_5
\end{bmatrix}
$$

$$
\begin{aligned}
\mathbf{Y}_1 =& [\ddot{\theta_{1r}}, \ddot{\theta_{1r}} + \ddot{\theta_{2r}}, \ddot{\theta_{1r}} + \ddot{\theta_{2r}} + \ddot{\theta_{3r}}, \\
& (2\ddot{\theta_{1r}} + 2\ddot{\theta_{2r}} + \ddot{\theta_{3r}})cos(\theta_3) - (\dot{\theta}_3(\dot{\theta_{1r}} + \dot{\theta_{2r}})(\dot{\theta}_1 + \dot{\theta}_2 + \dot{\theta}_3)\dot{\theta_{3r}})sin(\theta_3), \\
& - \ddot{y_{Pr}} sin(\theta_1) + \ddot{z_{Pr}} cos(\theta_1) + cos(\theta_1)g, \\
& - \ddot{y_{Pr}} sin(\theta_1 + \theta_2) + \ddot{z_{Pr}} cos(\theta_1 + \theta_2) + cos(\theta_1 + \theta_2)g, \\
& - \ddot{y_{Pr}} sin(\theta_1 + \theta_2 + \theta_3) + \ddot{z_{Pr}} cos(\theta_1 + \theta_2 + \theta_3) + cos(\theta_1 + \theta_2 + \theta_3)g, \\
& 0, \dot{\theta}_1, 0, 0, 0, \theta_1 - \theta_{10}, 0, 0] \\
\mathbf{Y}_2 =& [0, \ddot{\theta_{1r}} + \ddot{\theta_{2r}}, \ddot{\theta_{1r}} + \ddot{\theta_{2r}} + \ddot{\theta_{3r}}, \\
& (2\ddot{\theta_{1r}} + 2\ddot{\theta_{2r}} + \ddot{\theta_{3r}})cos(\theta_3) - (\dot{\theta}_3(\dot{\theta_{1r}} + \dot{\theta_{2r}}) + (\dot{\theta}_1 + \dot{\theta}_2 + \dot{\theta}_3)\dot{\theta_{3r}})sin(\theta_3), \\
& 0, -\ddot{y_{Pr}} sin(\theta_1 + \theta_2) + \ddot{z_{Pr}} cos(\theta_1 + \theta_2) + cos(\theta_1 + \theta_2)g, \\
& - \ddot{y_{Pr}} sin(\theta_1 + \theta_2 + \theta_3) + \ddot{z_{Pr}} cos(\theta_1 + \theta_2 + \theta_3) + cos(\theta_1 + \theta_2 + \theta_3)g, \\
& 0, 0, \dot{\theta}_2, 0, 0, 0, \theta_2 - \theta_{20}, 0] \\
\mathbf{Y}_3 =& [0, 0, \ddot{\theta_{1r}} + \ddot{\theta_{2r}} + \ddot{\theta_{3r}}, \\
& (\ddot{\theta_{1r}} + \ddot{\theta_{2r}})cos(\theta_3) - sin(\theta_3)(\dot{\theta}_1 + \dot{\theta}_2)(\dot{\theta_{1r}} + \dot{\theta_{2r}}), \\
& 0, 0, -\ddot{y_{rP}} sin(\theta_1 + \theta_2 + \theta_3) + (\ddot{z_{rP}} + g)cos(\theta_1 + \theta_2 + \theta_3), \\
& 0, 0, 0, \dot{\theta}_3, 0, 0, 0, \theta_3 - \theta_{30}] \\
\mathbf{Y}_4 =& [0, 0, 0, 0, (-sin(\theta_1)\ddot{\theta_{1r}} - cos(\theta_1)\dot{\theta}_1\dot{\theta_{1r}}), \\
& - sin(\theta_1 + \theta_2)(\ddot{\theta_{1r}} + \ddot{\theta_{2r}}) - cos(\theta_1 + \theta_2)(\dot{\theta}_1 + \dot{\theta}_2)(\dot{\theta_{1r}} + \dot{\theta_{2r}}), \\
& - sin(\theta_1 + \theta_2 + \theta_3)(\ddot{\theta_{1r}} + \ddot{\theta_{2r}} + \ddot{\theta_{3r}}) - cos(\theta_1 + \theta_2 + \theta_3)(\dot{\theta}_1 + \dot{\theta}_2 + \dot{\theta}_3)(\dot{\theta_{1r}} + \dot{\theta_{2r}} + \dot{\theta_{3r}}), \\
& \ddot{y_{Pr}}, 0, 0, 0, F_{bed,z} sign(\dot{y_P}), 0, 0, 0] \\
\mathbf{Y}_5 =& [0, 0, 0, 0, cos(\theta_1)\ddot{\theta_{1r}} - sin(\theta_1)\dot{\theta}_1\dot{\theta_{1r}}, \\
& cos(\theta_1 + \theta_2)(\ddot{\theta_{1r}} + \ddot{\theta_{2r}}) - sin(\theta_1 + \theta_2)(\dot{\theta}_1 + \dot{\theta}_2)(\dot{\theta_{1r}} + \dot{\theta_{2r}}), \\
& cos(\theta_1 + \theta_2 + \theta_3)(\ddot{\theta_{1r}} + \ddot{\theta_{2r}} + \ddot{\theta_{3r}}) - sin(\theta_1 + \theta_2 + \theta_3)(\dot{\theta}_1 + \dot{\theta}_2 + \dot{\theta}_3)(\dot{\theta_{1r}} + \dot{\theta_{2r}} + \dot{\theta_{3r}}), \\
& g + \ddot{z_{Pr}}, 0, 0, 0, 0, 0, 0, 0]
\end{aligned}
$$

Now the question is can the following equation be satisfied: $\mathbf{Q}_{nb}(\mathbf{q}, T_{v1}, T_{v2}, \theta_{v1}, \theta_{v2}) = Y\hat{\mathbf{a}} - K_D\mathbf{s}$? (where K_D is a constant, symmetric positive definite matrix) If so, the following can be done:

$$
\begin{aligned}
\dot{V} &= \mathbf{s}^T(Y\tilde{\mathbf{a}} - K_D\mathbf{s}) + \dot{\hat{\mathbf{a}}}^T P^{-1}\tilde{\mathbf{a}} \\
&= -\mathbf{s}^T K_D\mathbf{s} + \mathbf{s}^T Y\tilde{\mathbf{a}} + \dot{\hat{\mathbf{a}}}^T P^{-1}\tilde{\mathbf{a}}
\end{aligned}
$$

Then choose $\dot{\hat{\mathbf{a}}} = -PY^T\mathbf{s}$, so that $\dot{V} = -\mathbf{s}^T K_D\mathbf{s}$. Thererfore, $\dot{V} < 0, \forall \mathbf{s} \neq \mathbf{0}$ and $\dot{V} = 0$ when $\mathbf{s} = \mathbf{0}$. This ensures $\tilde{\mathbf{q}}, \dot{\tilde{\mathbf{q}}} = \mathbf{0}$ in steady state or in other words the generalized coordinates achieve their desired values.

Now returning to the question: Can $\mathbf{Q}_{nb}(\mathbf{q}, T_{v1}, T_{v2}, \theta_{v1}, \theta_{v2}) = Y\hat{\mathbf{a}} - K_D\mathbf{s}$? $\mathbf{Q}_{nb}$ is shown here:

$$\mathbf{Q}_{nb}(\mathbf{q}, T_{v1}, T_{v2}, \theta_{v1}, \theta_{v2})) = \begin{bmatrix} L_{av1}T_{v1}cos(\theta_1 - \theta_{v1}) + L_{av2}T_{v2}cos(\theta_{12} - \theta_{v2}) \\ L_{av2}T_{v2}cos(\theta_{12} - \theta_{v2}) \\ 0 \\ -T_{v1}s_{v1} - T_{v2}s_{v2} \\ T_{v1}c_{v1} + T_{v2}c_{v2} + F_{bed,z} \end{bmatrix}$$

It can be seen that forces $\mathbf{T}_{v1}$ and $\mathbf{T}_{v2}$ are heavily involved in $\mathbf{Q}_{nb}$. But controlling forces $\mathbf{T}_{v1}$ and $\mathbf{T}_{v2}$ directly is difficult and measuring those forces for feedback control is also difficult. Instead, consider the vines to be elastic with linear compliance equations. T_{v1} and T_{v2} can then be replaced with compliance equations such that $T_{v1} = T_{v1}(\theta_1, \theta_2, \theta_3, y_p, z_p | y_{v1}, z_{v1})$ and $T_{v2} = T_{v2}(\theta_1, \theta_2, \theta_3, y_p, z_p | y_{v2}, z_{v2})$. The inputs of the system then become positions: $y_{v1}, z_{v1}, y_{v2}, z_{v2}$. θ_{v1} and θ_{v2} can also be replaced by functions containing the generalized coordinates and new inputs. Under these substitutions: $\mathbf{Q}_{nb} = \mathbf{Q}_{nb}(\mathbf{q}, y_{v1}, z_{v1}, y_{v2}, z_{v2})$

$$\mathbf{Q}_{nb}(\mathbf{q}, y_{v1}, z_{v1}, y_{v2}, z_{v2}) = \begin{bmatrix} Q_{nb,1} \\ Q_{nb,2} \\ Q_{nb,3} \\ Q_{nb,4} \\ Q_{nb,5} \end{bmatrix}$$

where,

$$
\begin{aligned}
Q_{nb,1} &= -L_{av1}K_{v1}[((y_{v1} - y_p - L_{av1}c_1)^2 + (z_{v1} - z_p - L_{av1}s_1)^2)^{1/2} - L_{v10}] \\
&\cdot cos(\theta_1 - tan^{-1}(\frac{z_{v1} - z_p - L_{av1}s_1}{y_{v1} - y_p - L_{av1}c_1}) + \pi/2) \\
&- L_{av2}K_{v2}[((y_{v2} - y_p - L_{av2}c_{12})^2 + (z_{v2} - z_p - L_{av2}s_{12})^2)^{1/2} - L_{v20}] \\
&\cdot cos(\theta_{12} - tan^{-1}(\frac{z_{v2} - z_p - L_{av2}s_{12}}{y_{v2} - y_p - L_{av2}c_{12}}) + \pi/2) \\
Q_{nb,2} &= -L_{av2}K_{v2}[((y_{v2} - y_p - L_{av2}c_{12})^2 + (z_{v2} - z_p - L_{av2}s_{12})^2)^{1/2} - L_{v20}] \\
&\cdot cos(\theta_{12} - tan^{-1}(\frac{z_{v2} - z_p - L_{av2}s_{12}}{y_{v2} - y_p - L_{av2}c_{12}}) + \pi/2) \\
Q_{nb,3} &= 0 \\
Q_{nb,4} &= K_{v1}[((y_{v1} - y_p - L_{av1}c_1)^2 + (z_{v1} - z_p - L_{av1}s_1)^2)^{1/2} - L_{v10}] \\
&\cdot sin(tan^{-1}(\frac{z_{v1} - z_p - L_{av1}s_1}{y_{v1} - y_p - L_{av1}c_1} - \pi/2) \\
&+ K_{v2}[((y_{v2} - y_p - L_{av2}c_{12})^2 + (z_{v2} - z_p - L_{av2}s_{12})^2)^{1/2} - L_{v20}] \\
&\cdot sin(tan^{-1}(\frac{z_{v2} - z_p - L_{av2}s_{12}}{y_{v2} - y_p - L_{av2}c_{12}}) - \pi/2) \\
Q_{nb,5} &= -K_{v1}[((y_{v1} - y_p - L_{av1}c_1)^2 + (z_{v1} - z_p - L_{av1}s_1)^2)^{1/2} - L_{v10}] \\
&\cdot cos(tan^{-1}(\frac{z_{v1} - z_p - L_{av1}s_1}{y_{v1} - y_p - L_{av1}c_1} - \pi/2) \\
&- K_{v2}[((y_{v2} - y_p - L_{av2}c_{12})^2 + (z_{v2} - z_p - L_{av2}s_{12})^2)^{1/2} - L_{v20}] \\
&\cdot cos(tan^{-1}(\frac{z_{v2} - z_p - L_{av2}s_{12}}{y_{v2} - y_p - L_{av2}c_{12}}) - \pi/2) \\
&+ F_{bed,z}
\end{aligned}
$$

and, L_{v10} and L_{v20} are the unstretched lengths of vines 1 and 2, respectively.

Ignoring the zero entry in $\mathbf{Q}_{nb}(\mathbf{q}, y_{v1}, z_{v1}, y_{v2}, z_{v2})$, gives 4 nonlinear equations and 4 inputs to solve for $(y_{v1}, z_{v1}, y_{v2}, z_{v2})$. This is a well-defined system of equations. Ignoring the zero entry in $\mathbf{Q}_{nb}$ relinquishes the ability to control θ_3 at all because the third row on $\mathbf{Q}_{nb}$ are the generalized forces acting on θ_3. This is the same situation as in 2 and it is still appropriate for the reasons stated in section 2.2.

$$
\mathbf{Q}'_{nb}(\mathbf{q}, y_{v1}, z_{v1}, y_{v2}, z_{v2}) = \begin{bmatrix} Q_{nb,1} \\ Q_{nb,2} \\ Q_{nb,4} \\ Q_{nb,5} \end{bmatrix} = Y'\hat{\mathbf{a}} - K'_D\mathbf{s}
$$

where Y' is Y with the third row omitted and K'_D is K_D with the third row omitted. $\mathbf{s}'$ will be used below and represents $\mathbf{s}$ with the third row omitted.

MATLAB can be used to solve the nonlinear system of equations: $\mathbf{F}(\mathbf{q}, \dot{\mathbf{q}}, y_{v1}, z_{v1}, y_{v2}, z_{v2}) = \mathbf{Q}'_{nb} - (Y'\hat{\mathbf{a}} - K'_D\mathbf{s}) = \mathbf{0}$ for the system inputs $y_{v1}, z_{v1}, y_{v2}, z_{v2}$. Let the solution to the inputs be $\bar{y_{v1}}, \bar{z_{v1}}, \bar{y_{v2}}, \bar{z_{v2}}$. This solution may not perfectly solve $\mathbf{F} = \mathbf{0}$. Instead $\mathbf{F}(\mathbf{q}, \dot{\mathbf{q}}, \bar{y_{v1}}, \bar{z_{v1}}, \bar{y_{v2}}, \bar{z_{v2}}) = \mathbf{e} \neq \mathbf{0}$, where $\mathbf{e}$ is the residual error. The residual error enters the adaptive control formulation in the following way.

$$
\begin{aligned}
\dot{V} &= \mathbf{s}'^T(\mathbf{Q}'_{nb} - Y'\mathbf{a}) + \dot{\hat{\mathbf{a}}}^T P^{-1}\tilde{\mathbf{a}} \\
&= \mathbf{s}'^T(Y'\tilde{\mathbf{a}} - K'_D\mathbf{s}' + \mathbf{e}) + \dot{\hat{\mathbf{a}}}^T P^{-1}\tilde{\mathbf{a}} \\
&= -\mathbf{s}'^T K_D\mathbf{s}' + \mathbf{s}'^T Y\tilde{\mathbf{a}} + \mathbf{s}'^T\mathbf{e} + \dot{\hat{\mathbf{a}}}^T P^{-1}\tilde{\mathbf{a}}
\end{aligned}
$$

Let $\dot{\hat{\mathbf{a}}} = -PY^T\mathbf{s}'$, then

$$
\dot{V} = -\mathbf{s}'^T K_D\mathbf{s} + \mathbf{s}'^T\mathbf{e}
$$

3.4 Results

In simulation, $\mathbf{e}$ doesn't pose to be a problem all the time and there are solutions to minimize it. One such solution is for every step of the adaptive control the jacobian of the objective function $\mathbf{F}$ with respect to the system inputs $y_{v1}, z_{v1}, y_{v2}, z_{v2}$: $\frac{\partial \mathbf{F}}{\partial [y_{v1}, z_{v1}, y_{v2}, z_{v2}]}$, is made sure to be non-singular. This is to make sure that the inputs chosen as the solution to the objective function are stable and not in a singular orientation.

The same test that was executed for quasi-static control is executed for adaptive control. The results are shown in the figures below. The parameter vector $\hat{\mathbf{a}}$ was initialized at -50% error from the actual parameter values. The unstretched lengths of the straps are 0.5m.

Even though these results shown in Figure 3.3 look good, the position of v_2 does not make physical sense. The control theorem puts v_2 under thigh, such that strap seems to be pushing against the thigh, rather than pulling. If this was to happen in real-life, the strap would go slack rather than provide any pushing force. Figure 3.4 shows a snapshot of this behavior.

More research needs to be conducted to understand this phenomenon and fix it, so that the control will make physical sense and work on a physical system. In addition, more research into improvement of desired $F_{bed,z}$ tracking is needed.

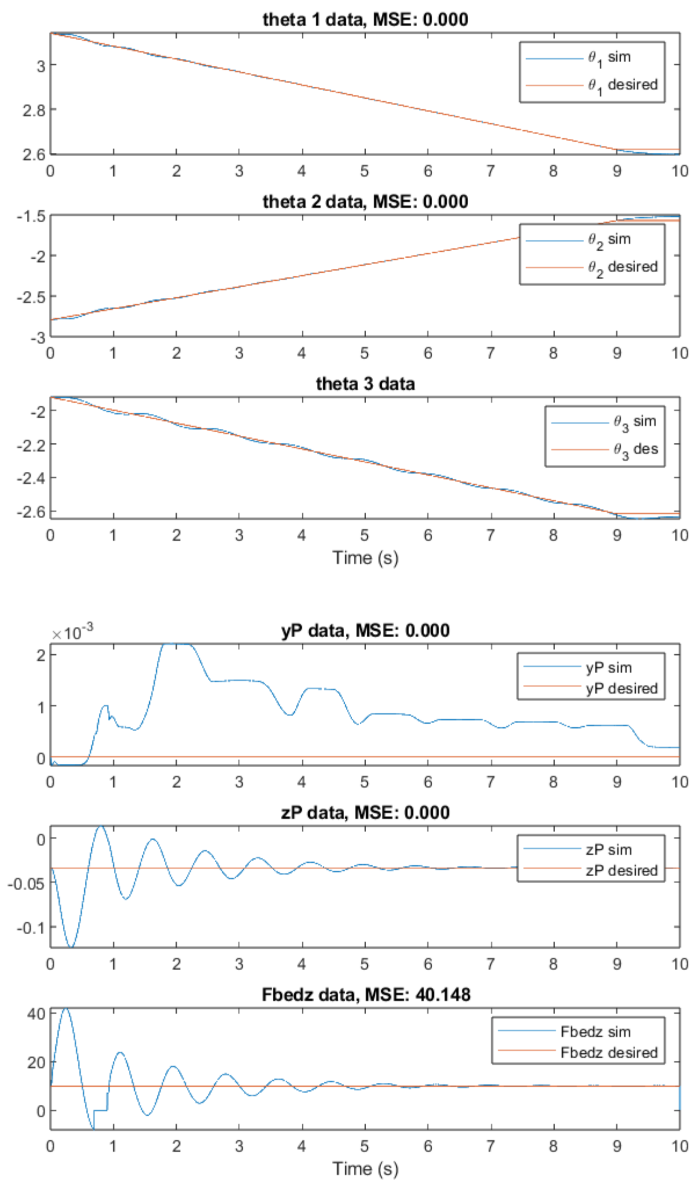

Figure 3.3: Adaptive control results. Mean squared error is shown at the top of each graph.

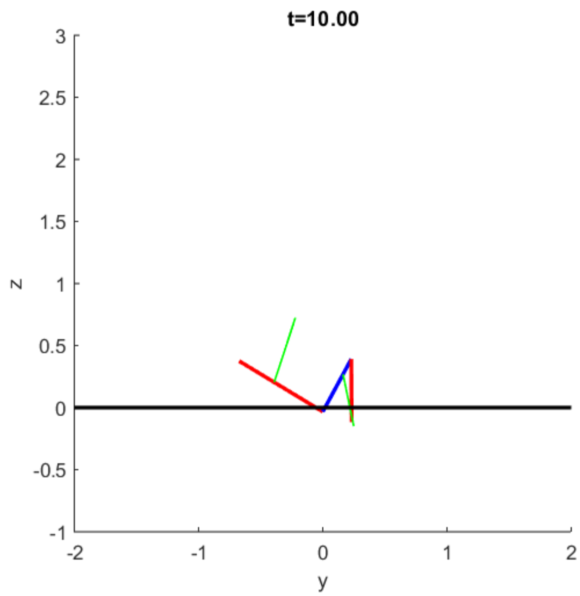

Figure 3.4: Snapshot of adaptive control simulation animation. The free end of the strap attached to the thigh is under the thigh.

Chapter 4

Conclusion

Patients with prolonged bed rest, which can happen due to a variety of reasons, are in danger of deterioration of important bodily systems, muscle loss, skin breakdown, and more adverse effects. Caregivers are employed to help prevent these issues. However in trying to promote mobility of these patients caregivers continue to sustain injuries. In fact, there are more injuries in caregiving than in manufacturing and construction industries. Assistive devices were created to prevent caregiver injuries, but there are various factors that occur in industry that prevent the usage of the most common assistive devices. Automating mobilization of bedridden patients is the solution. This thesis presented two versions of control theory that can be used to automate in-bed movement and repositioning, assistance to a seated position, and transfer out of the bed for patients with severe immobility. Both the quasi-static closed loop control and the adaptive control are able to control the hip and thigh angles, and hip position well. The control of the normal force on this hip from the bed is currently inaccurate. Though more research needs to be done to improve the performance of the controllers, the results show promise that a truly automated solution exists. Furthermore, future work on an improved mechanism that can control the straps, instead of robotic arms, would open up the range of motions of the straps and therefore the controllable motions of the patient.

References

[1] K. Ernstmeyer and E. Christman, *Nursing Fundamentals*. Open Resources for Nursing (Open RN), 2021, ch. Chapter 13 Mobility. URL: https://www.ncbi.nlm.nih.gov/books/NBK591828/.

[2] C. R. R. Bilal Orun and D. Martins. "Review of assistive technologies for bedridden persons." (Nov. 2015), URL: https://www.researchgate.net/publication/283459329_Review_of_assistive_technologies_for_bedridden_persons.

[3] H. J. L. Ashley L. Schoenfisch Kristen L. Kucera, J. McIlvaine, L. Becherer, T. James, and S. Avent, "Use of assistive devices to lift, transfer, and reposition hospital patients," *Nursing Research*, vol. 68, no. 1, pp. 3–12, Feb. 2019. DOI: https://doi.org/10.1097/nnr.0000000000000325.

[4] H. Wang and F. Kasagami, "A patient transfer apparatus between bed and stretcher," *IEEE Transactions on Systems, Man, and Cybernetics, Part B (Cybernetics)*, vol. 38, pp. 60–67, Feb. 2008. DOI: 10.1109/TSMCB.2007.909442.

[5] W. Finger and H. Asada, "Design and control of an active mattress for moving bedridden patients," in *Proceedings 1999 IEEE International Conference on Robotics and Automation*, 1999. DOI: 10.1109/ROBOT.1999.770408. URL: https://ieeexplore.ieee.org/document/770408.

[6] A. B. B. Roy and H. Asada, "Maneuvering a bed sheet for repositioning a bedridden patient," *2003 IEEE International Conference on Robotics and Automation*, 2003. DOI: 10.1109/ROBOT.2003.1241924. URL: https://ieeexplore.ieee.org/document/1241924.

[7] S.-W. Peng and F.-L. Lian, "Mechanism design and mechatronic control of a multifunctional test bed for bedridden healthcare," *IEEE/ASME TRANSACTIONS ON MECHATRONICS*, vol. 15, no. 2, pp. 234–241, May 2010. DOI: 10.1109/TMECH.2009.2021470.

[8] C. O. Kap-Ho Seo Tae-Yong Choi, "Development of a robotic system for the bedridden," *Mechatronics*, vol. 21, pp. 227–238, 2011. URL: https://www.academia.edu/106051268/Development_of_a_robotic_system_for_the_bed_ridden.

[9] H. N. Toshiharu Mukai Shinya Hirano, Y. Kato, Y. Sakaida, S. Guo, and S. Hosoe, "Development of a nursing-care assistant robot riba that can lift a human in its arms," *2010 IEEE/RSJ International Conference on Intelligent Robots and Systems*, Oct. 2010. DOI: 10.1109/IROS.2010.5651735. URL: https://ieeexplore.ieee.org/document/5651735.

[10] J.-J. E. Slotine and W. Li, *Applied Nonlinear Control*. Prentice-Hall, Inc., 1991.